Electronic Supplementary Material (ESI) for New Journal of Chemistry.

Supporting Information

Theoretical Study of the Strain Effect on the Oxygen Reduction Reaction Activity and Stability of FeNC Catalyst

Xiaoming Zhang[a], Zhangxun Xia[a], Huanqiao Li[a], Shansheng Yu[b], Suli Wang[a], Gongquan Sun[a]**

[a]Division of Fuel Cells and Battery, Dalian National Laboratory for Clean Energy, Dalian Institute of Chemical Physics, Chinese Academy of Sciences, Dalian, China 116023

[b]Department of Materials Science, Jilin University, Changchun 130012, PR China

The thermodynamics of the ORR

Three possible four electrons overall reaction pathways (the associative and dissociative mechanisms) of O_2 reducing to H_2O in an acid environment is $O_2 + 4H^+ + 4e^- \rightarrow 2H_2O$ (l), which includes.

The ORR occurs on Fe atom:

Mechanism I:

$$* + O_2(g) + 4H^+ + 4e^- \rightarrow *OOH + 3H^+ + 3e^- \quad (S1)$$

$$*OOH + 3H^+ + 3e^- \rightarrow *O + 2H^+ + 2e^- + H_2O\ (l) \quad (S2)$$

$$*O + 2H^+ + 2e^- \rightarrow *OH + H^+ + e^- \quad (S3)$$

$$*OH + H^+ + e^- \rightarrow * + H_2O\ (l) \quad (S4)$$

Mechanism II:

$$* + O_2(g) + 4H^+ + 4e^- \rightarrow *OOH + 3H^+ + 3e^- \quad (S5)$$

$$*OOH + 3H^+ + 3e^- \rightarrow 2*OH + 2H^+ + 2e^- \quad (S6)$$

$$2*OH + 2H^+ + 2e^- \rightarrow *OH + H^+ + e^- + H_2O\ (l) \quad (S7)$$

$$*OH + H^+ + e^- \rightarrow * + H_2O\ (l) \quad (S8)$$

Mechanism III:

$$* + O_2(g) + 2H^+ + 2e^- \rightarrow *OOH + 2H^+ + 2e^- \quad (S9)$$

$$*OOH + H^+ + e^- \rightarrow H_2O_2* \quad (S10)$$

The ORR occurs on Fe atom and adjacent C:

Mechanism IV:

$$* + {}^{\#} + O_2(g) + 4H^+ + 4e^- \rightarrow *OOH + 3H^+ + 3e^- \quad (S11)$$

$$*OOH + {}^{\#} + 3H^+ + 3e^- \rightarrow *O + {}^{\#}OH + 3H^+ + 3e^- \quad (S12)$$

$$*O + {}^{\#}OH + 3H^+ + 3e^- \rightarrow *OH + {}^{\#}OH + {}^{\#} + 2H^+ + 2e^- \quad (S13)$$

$$*OH + {}^{\#}OH + 2H^+ + 2e^- \rightarrow *OH + H^+ + e^- + H_2O\ (l) \quad (S14)$$

$$*OH + H^+ + e^- \rightarrow * + H_2O\ (l) \quad (S15)$$

Mechanism V:

$$* + {}^{\#} + O_2(g) + 4H^+ + 4e^- \rightarrow *OOH + 3H^+ + 3e^- \quad (S16)$$

$$*OOH + {}^{\#} + 3H^+ + 3e^- \rightarrow *O + {}^{\#}OH + 3H^+ + 3e^- \quad (S17)$$

$$*O + {}^{\#}OH + 3H^+ + 3e^- \rightarrow *O + H_2O\ (l) + {}^{\#} + 2H^+ + 2e^- \quad (S18)$$

$$*O + 2H^+ + 2e^- \rightarrow *OH + H^+ + e^- \quad \text{(S19)}$$

$$*OH + H^+ + e^- \rightarrow * + H_2O\ (l) \quad \text{(S20)}$$

Mechanism VI:

$$* + {}^{\#} + O_2(g) + 4H^+ + 4e^- \rightarrow *O_2 + 4H^+ + 4e^- \quad \text{(S21)}$$

$$*O_2 + 4H^+ + 4e^- \rightarrow *O + {}^{\#}O + 4H^+ + 4e^- \quad \text{(S22)}$$

$$*O + {}^{\#}O + 4H^+ + 4e^- \rightarrow *O + {}^{\#}OH + 3H^+ + 3e^- \quad \text{(S23)}$$

$$*O + {}^{\#}OH + 3H^+ + 3e^- \rightarrow *O + H_2O\ (l) + {}^{\#} + 2H^+ + 2e^- \quad \text{(S24)}$$

$$*O + 2H^+ + 2e^- \rightarrow *OH + H^+ + e^- \quad \text{(S25)}$$

$$*OH + H^+ + e^- \rightarrow * + H_2O\ (l) \quad \text{(S26)}$$

where * and # refers to Fe and C active site in FeN_4 model. (l) and (g) refer to the liquid and gas phases, respectively. *O, *OH and *OOH are the adsorbed intermediates.

For each step, the reaction free energy ΔG is defined as the difference between free energies of the initial and final states and is given by the expression[1],

$$\Delta G = \Delta E + \Delta ZPE - T\Delta S + \Delta G_U + \Delta G(pH) \quad \text{(S27)}$$

That is:

$$\Delta G_1 = \Delta G_{OOH^*} - 4.92eV - \Delta G_{H^+}(pH) + eU \quad \text{(S28)}$$

$$\Delta G_2 = \Delta G_{O^*} - \Delta G_{OOH^*} - \Delta G_{H^+}(pH) + eU \quad \text{(S29)}$$

$$\Delta G_3 = \Delta G_{OH^*} - \Delta G_{O^*} - \Delta G_{H^+}(pH) + eU \quad \text{(S30)}$$

$$\Delta G_4 = -\Delta G_{OH^*} - \Delta G_{H^+}(pH) + eU \quad \text{(S31)}$$

$$\Delta G_6 = \Delta G_{2OH^*} - \Delta G_{OOH^*} - \Delta G_{H^+}(pH) + eU \quad \text{(S32)}$$

$$\Delta G_7 = \Delta G_{2OH^*} - \Delta G_{2\ ^*OH} - \Delta G_{H^+}(pH) + eU \quad \text{(S33)}$$

$$\Delta G_{10} = \Delta G_{H_2O_2^*} - \Delta G_{OOH^*} - \Delta G_{H^+}(pH) + eU \quad \text{(S34)}$$

$$\Delta G_{12} = \Delta G_{O^*} + \Delta G_{OH^*} - \Delta G_{OOH^*} \quad \text{(S35)}$$

$$\Delta G_{13} = (\Delta G_{OH^{\#}} + \Delta G_{OH^*}) - (\Delta G_{OH^{\#}} + \Delta G_{O^*}) - \Delta G_{H^+}(pH) + eU \quad \text{(S36)}$$

$$\Delta G_{14} = \Delta G_{OH^*} - (\Delta G_{OH^\#} + \Delta G_{OH^*}) - \Delta G_{H^+}(pH) + eU \quad \text{(S37)}$$

$$\Delta G_{18} = \Delta G_{O^*} - (\Delta G_{OH^\#} + \Delta G_{O^*}) - \Delta G_{H^+}(pH) + eU \quad \text{(S38)}$$

$$\Delta G_{22} = (\Delta G_{O^\#} + \Delta G_{O^*}) - 4.92 \quad \text{(S39)}$$

$$\Delta G_{23} = (\Delta G_{OH^\#} + \Delta G_{O^*}) - (\Delta G_{O^\#} + \Delta G_{O^*}) - \Delta G_{H^+}(pH) + eU \quad \text{(S19)}$$

The Gibbs free energies are related to the adsorption energies of the various intermediate species. The adsorption free energy changes of these intermediate species are determined using $\Delta G_{ads} = \Delta E_{ads}^{DFT} + \Delta ZPE - T\Delta S$, where ΔE_{ads}^{DFT} can be calculated relative to H_2O and H_2 (The absorption energies were calculated as follows[2], $\Delta E_{OH^*} = E(OH^*) - E(*) - (E_{H_2O} - 1/2E_{H_2})$, $\Delta E_{OOH^*} = E(OOH^*) - E(*) - (2E_{H_2O} - 3/2E_{H_2})$, $\Delta E_{O^*} = E(O^*) - E(*) - (E_{H_2O} - E_{H_2})$), ΔZPE and TΔS are the zero point energy difference and the entropy change between the absorbed state and the free state, i.e., the gas phase (listed in Table S2), respectively, and T is the temperature (298.15 K in this work). e is the elementary charge and U is the potential difference between the electrode and the normal hydrogen electrode (NHE). The free energy change of H^+ is derived according to $\Delta G(pH) = k_B T ln(10) \times \mathrm{pH}$, ($k_B$ is Boltzmann's constant, and pH = 1). Because the high-spin ground state of an oxygen molecule is difficult to describe in DFT calculations, the free energy of O_2(g) is derived as $G_{O_2}(g) = 2G_{H_2O}(l) - 2G_{H_2}(g)$. Additionally, the activation energy barrier (ΔE_b) is defined as the difference between the energy of the transition structures (E_{TS}) and the initial structures (E_{IS}), $\Delta E_b = E_{TS} - E_{IS}$.

Figures and Tables

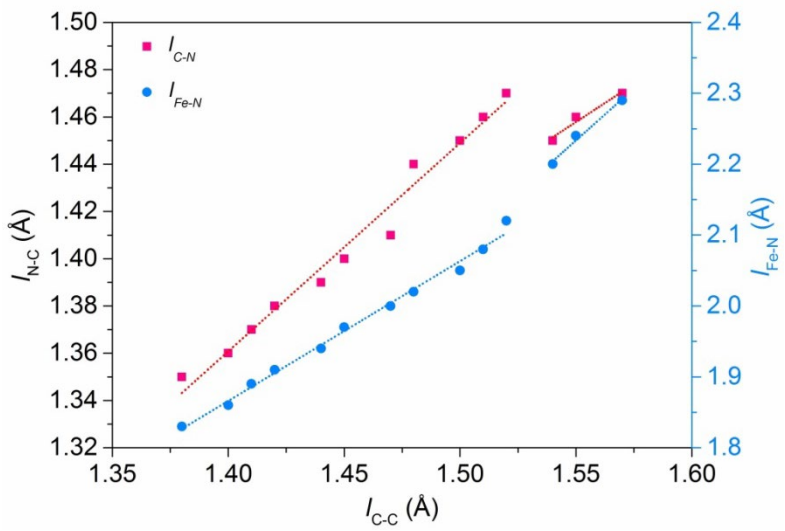

Figure S 1 The bond length of C-N and Fe-N in FeNC under various stress.

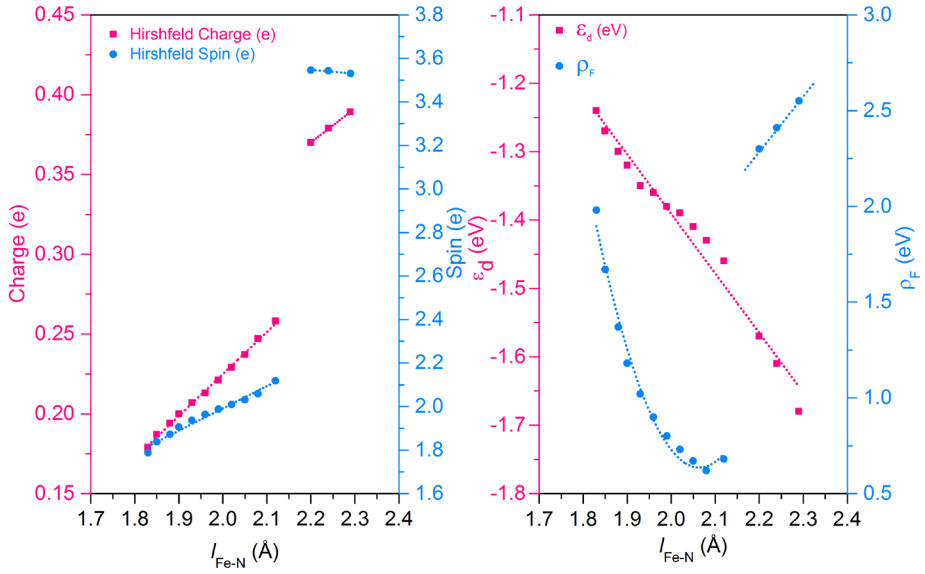

Figure S 2 The electronic properties of FeNC electrocatalyst under stress: (a) Hirshfeld Charge and spin, (b) d band center and density of states at Fermi level.

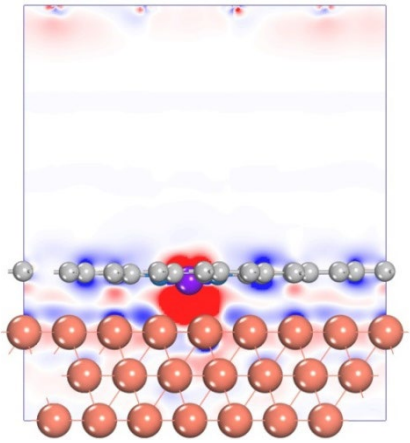

Figure S 3 The charge density difference for Cu@FeNC. The isosurface value is 0.005 e/Å^3. The red colour represents electron accumulation, while the blue colour represents electron depletion. The intensity of colour depends on the amount of electron change: the darkest red marks the most accumulation; the darkest blue marks the most depletion. Gray, carbon atom; Blue, nitrogen atom; Purple, Fe atom; Yellow, Cu atom.

Table S 1 Bond length of initial C-C in graphene and optimized Fe-N, C-N in FeNC

Strain	$l_{C\text{-}C}$ (Å)	$l_{C\text{-}N}$(Å)	$l_{Fe\text{-}N}$(Å)
-3.0%	1.38	1.35	1.83
-2.0%	1.40	1.36	1.86
-1.0%	1.41	1.37	1.89
0.0%	1.42	1.38	1.91
1.0%	1.44	1.39	1.94
2.0%	1.45	1.40	1.97
3.0%	1.47	1.41	2.00
4.0%	1.48	1.44	2.02
5.0%	1.50	1.45	2.05
6.0%	1.51	1.46	2.08
7.0%	1.52	1.47	2.12
8.0%	1.54	1.45	2.20
9.0%	1.55	1.46	2.24
10.0%	1.57	1.47	2.29

Table S 2 The zero point energies and entropic corrections of oxygenates at 298.15 K

Species	ZPE[3]	TS[3]	ZPE[4]	TS[4]	ZPE[5]	TS[5]	ZPE*	TS*
O*	0.07	0.00	0.05	0.00	0.084	0.05	0.05	0.05
OH*	0.36	0.00	0.36	0.06	0.386	0.07	0.37	0.10
OOH*	0.39	0.00	0.40	0.08	0.457	0.16	0.46	0.16
O_2	-	-	0.11	0.64	-	-	-	-
H_2	0.27	0.41	0.27	0.41	0.27	0.41	0.27	0.41
H_2O	0.56	0.67	0.56	0.67	0.56	0.67	0.56	0.67

*The present work.

Table S 3 The geometric properties, electronic properties (d band center, density of states at Fermi level, Hirshfelf charge and Hirshfelf spin) and adsorption free energy (eV) of strained FeNC.

Sample	l_{Fe-N}	Charge	Spin	ε_d	ρ_F	l_{Fe-O}	ΔG_{*OH}
-3%	1.83	0.179	1.788	-1.24	1.98	1.85	0.09
-2%	1.85	0.187	1.838	-1.27	1.67	1.84	0.41
-1%	1.88	0.194	1.872	-1.30	1.37	1.84	0.54
0%	1.90	0.200	1.906	-1.32	1.18	1.84	0.62
1%	1.93	0.207	1.937	-1.35	1.02	1.84	0.67
2%	1.96	0.213	1.964	-1.36	0.90	1.83	0.71
3%	1.99	0.221	1.988	-1.38	0.80	1.80	0.75
4%	2.02	0.229	2.010	-1.39	0.73	1.83	0.78
5%	2.05	0.237	2.031	-1.41	0.67	1.80	0.80
6%	2.08	0.247	2.059	-1.43	0.62	1.80	0.82
7%	2.12	0.258	2.118	-1.46	0.68	1.82	0.78
8%	2.20	0.370	3.546	-1.57	2.30	1.85	0.37
9%	2.24	0.379	3.543	-1.61	2.41	1.85	0.35
10%	2.29	0.389	3.530	-1.68	2.55	1.84	0.30

References

1. He, F.; Li, K.; Yin, C.; Wang, Y.; Tang, H.; Wu, Z., Single Pd atoms supported by graphitic carbon nitride, a potential oxygen reduction reaction catalyst from theoretical perspective. *Carbon* **2017,** *114*, 619-627.
2. Schaub, R.; Thostrup, P.; Lopez, N.; Laegsgaard, E.; Stensgaard, I.; Norskov, J. K.; Besenbacher, F., Oxygen vacancies as active sites for water dissociation on rutile TiO(2)(110). *Phys Rev Lett* **2001,** *87* (26), 266104.
3. Ling, C.; Shi, L.; Ouyang, Y.; Zeng, X. C.; Wang, J., Nanosheet Supported Single-Metal Atom Bifunctional Catalyst for Overall Water Splitting. *Nano Lett* **2017,** *17* (8), 5133-5139.
4. Zhou, S.; Liu, N. S.; Wang, Z. Y.; Zhao, J. J., Nitrogen-Doped Graphene on Transition Metal Substrates as Efficient Bifunctional Catalysts for Oxygen Reduction and Oxygen Evolution Reactions. *Acs Applied Materials & Interfaces* **2017,** *9* (27), 22578-22587.
5. Li, M. T.; Zhang, L. P.; Xu, Q.; Niu, J. B.; Xia, Z. H., N-doped graphene as catalysts for oxygen reduction and oxygen evolution reactions: Theoretical considerations. *Journal of Catalysis* **2014,** *314*, 66-72.